CONNECTING GEOMETRY, TOPOLOGY AND SPECTRA FOR FINITE-GAP NLS POTENTIALS

Annalisa M. Calini
Dept. of Mathematics, College of Charleston, Charleston, SC 29424
calinia@cofc.edu
and
Thomas A. Ivey
Dept. of Mathematical Sciences, Ball State University, Muncie IN 47306
tivey@math.bsu.edu

Abstract. Using the connection between closed solution curves of the vortex filament flow and quasiperiodic solutions of the nonlinear Schrödinger equation (NLS), we relate the knot types of finite-gap solutions to the Floquet spectra of the corresponding NLS potentials, in the special case of small amplitude curves close to multiply-covered circles.

1. Introduction

The first, and perhaps richest, example of connection between curve evolution and soliton equations [7] is provided by the vortex filament flow, or localized induction equation (LIE)

$$\gamma_t = \gamma_x \times \gamma_{xx}, \tag{1}$$

where t is time and γ is a curve in $\mathbb{R}^3$ with arclength coordinate x, and the associated cubic focusing nonlinear Schrödinger equation (NLS)

$$iq_t + q_{xx} + 2|q|^2 q = 0. \tag{2}$$

In the same year that the complete integrability of the NLS equation was established by Zakharov and Shabat [12], Hasimoto [9] discovered a transformation which constructs the complex NLS potential $q(x,t)$ in terms of the curvature and torsion of the evolving curve, thus adding the vortex filament flow to the growing number of completely integrable PDE's.

When periodic boundary conditions are imposed, solutions of the LIE are closed, and possibly knotted, curves evolving in three-dimensional space. Among them, the large class of closed filaments coming from finite-gap NLS potentials (periodic and quasi-periodic analogues of multi-solitons) are particularly interesting. On the one hand, such curves can be explicitly constructed using the theory of Baker-Akheizer functions on hyperelliptic Riemann surfaces whose branch points are part of the Floquet spectrum of the associated NLS potentials. (Not all finite-gap curves are closed, however Grinevich and Schmidt [8] recently gave a precise characterization of which spectra give rise to closed curves.) On the other hand, finite-gap solutions of the LIE, as opposed to more general solutions, are good candidates for knot representatives since, at least for low number of phases, their topology appears to be preserved by the time evolution. One then hopes that the knot type of closed finite-gap solutions can be described using tools from integrable systems, such as Floquet theory and Bäcklund transformations.

This work considers closed LIE curves coming from periodic finite-gap NLS solutions close to modulationally unstable plane waves, and investigates the relation between their topological and geometrical properties and the Floquet spectra of the associated NLS potentials. In this case, both the expression for $\gamma(x,t)$ and the Floquet spectrum can be computed using perturbation techniques. Although a complete understanding of the relation between knot types and spectra of finite-gap curves may require the Baker function representation, the perturbation analysis done here yields several interesting results.

The spectrum of a modulationally unstable plane wave (shown in Figure 1) contains a finite number of imaginary double points labelling its linear instabilities. It is well-known that the homoclinic manifold of an unstable NLS solution can be explicitly constructed using Bäcklund transformations. In previous work [3], the first author computed the LIE curves associated with homoclinic orbits of unstable plane waves: these curves are singular knots whose self-intersections persist throughout the time evolution. Since homoclinic orbits are degenerate finite-gap solutions (associated with singular Riemann surfaces), one can ask whether the corresponding singular knots separate curves of different knot types. We will give a positive answer to this question for a few low-genus cases.

The article begins with a description of the Hasimoto transformation and its inverse, followed in Section 3 by a review of basic facts about Floquet theory, with a modulationally unstable plane wave (associated with a multiply covered circle) as illustrative example. Section 3 also describes some connections between the geometry of curves associated with finite-gap NLS potentials and their Floquet spectra; in particular, it contains an interpretation of the Grinevich-Schmidt closure condition, and a description of the geometry of curves coming from three-phase solutions whose spectra have the even symmetry $\lambda \to -\lambda$.

In Section 4, we introduce a trigonometric perturbation of the unstable plane wave potential containing modulationally unstable modes, which causes one or more imaginary double points to split and form a gap or a complex band in the associated spectrum. This kind of perturbation was used in the work of Ablowitz, Herbst and Schober [1] to give a qualitative description of the Floquet spectrum of nearby finite-gap solutions. We extend this computation to the perturbation expansion for the position vector of the curve, which turns out to be closed up to second order in ϵ. The truncated expression at $O(\epsilon)$ is then a closed curve of the same knot type as a nearby closed curve whose Floquet spectrum is an $O(\epsilon^2)$-perturbation of the perturbed plane wave spectrum. One can thus relate the perturbed plane wave spectrum to the topology of the truncated curve.

In Section 5 we prove constructively that generic first order perturbations which cause a single imaginary double point to undergo an asymmetric splitting and leave all other critical points unaffected to $O(\epsilon)$ are associated with torus knots of types determined by which double point is selected by the perturbation.

Section 6 contains experiments in which the explicit relation between spectra and knot types is explained, both in the even case where singular knots arise, and in the noneven case. In the latter case, when a single imaginary double point is selected by the perturbation, the handedness of the resulting torus knot is shown to be related to the sign of the velocity of the associated perturbed potential (a modulated travelling wave solution).

When the perturbation contains two unstable modes whose frequencies are relatively prime multiples of the basic frequency (thus causing two imaginary double points to split at first order), a most interesting result occurs: the associated curve is a cable knot, whose precise type is described at the end of the section. This is the first time the knot type of one of the higher phase solutions of the LIE (a modulated 4-phase solution) is explicitly computed.

2. The Hasimoto map and its inverse

Hasimoto [9] first observed that solutions of the vortex filament flow (1) induce solutions of the NLS equation (2) of the form

$$q(x,t) = \frac{1}{2}\kappa(x,t)\exp\left[i\int^x \tau(s,t)\right] ds \tag{3}$$

where κ and τ are the curvature and torsion of the evolving space curve. (Potential q is defined up to multiplication by a unit modulus constant.)

An inverse to the Hasimoto map is defined using solutions of the AKNS linear system which facilitates the solution of NLS by inverse scattering. In fact, since the time dependence of finite-gap solutions is through linear phases, we only need the spatial part of the Lax pair:

$$\psi_x = \begin{pmatrix} i\lambda & q(x) \\ -\bar{q}(x) & -i\lambda \end{pmatrix}\psi, \qquad \lambda \in \mathbb{C}. \tag{4}$$

Let $\Psi(x;\lambda)$ be a fundamental matrix solution of this system; note that Ψ takes values in the Lie group $SU(2)$ when $\lambda \in \mathbb{R}$. Following Sym [11], we define

$$\gamma(x;\lambda) = \Psi^{-1}\frac{d\Psi}{d\lambda}, \qquad \lambda \in \mathbb{R}. \tag{5}$$

Matrix γ takes value in the Lie algebra $su(2)$, which we identify with $\mathbb{R}^3$ by fixing an isometry taking the standard metric to minus one half of the Killing form, and taking the Lie bracket to twice the cross product. Now we regard γ as a space curve, with unit tangent vector given by

$$\gamma_x = \Psi^{-1}\begin{pmatrix} i & 0 \\ 0 & -i \end{pmatrix}\Psi. \tag{6}$$

Further differentiation shows that the curvature and torsion of $\gamma(x;0)$ are related to q by the Hasimoto correspondence (3). (In general, $\gamma(x;\lambda)$ has the same curvature as $\gamma(x;0)$, but the torsion changes by an additive constant.)

It is instructive to carry out this construction beginning with the constant plane wave potential $q(x) = a$, for which

$$\Psi(x;\lambda) = P \begin{pmatrix} e^{ikx} & 0 \\ 0 & e^{-ikx} \end{pmatrix} P^{-1}, \qquad P = \begin{pmatrix} 1 & 1 \\ \frac{i}{a}(k-\lambda) & -\frac{i}{a}(k+\lambda) \end{pmatrix}, \tag{7}$$

where $k = \sqrt{\lambda^2 + a^2}$. Fixing an oriented orthonormal basis for $su(2) \cong \mathbb{R}^3$

$$\mathbf{e}_1 = \begin{pmatrix} i & 0 \\ 0 & -i \end{pmatrix}, \ \mathbf{e}_2 = \begin{pmatrix} 0 & i \\ i & 0 \end{pmatrix}, \ \mathbf{e}_3 = \begin{pmatrix} 0 & -1 \\ 1 & 0 \end{pmatrix},$$

we find that γ is a circle of diameter $1/a$:

$$\gamma(x) = [\mathbf{e}_1 \sin 2ax + \mathbf{e}_2(1 - \cos 2ax)]/(2a).$$

Multiply-covered versions of this circle will be perturbed to generate a variety of knots in section 4 below.

3. Geometry and spectra for finite-gap potentials

In this section we discuss the relationship between the geometry of a space curve γ and the spectrum of the potential q associated to it by the Hasimoto map.

First, suppose q is periodic with period L. The spectrum $\sigma(q)$ is defined to be the set of values of the complex parameter λ for which there exist bounded eigenfunctions of the linear system (4). The symmetries of this linear system imply that $\sigma(q)$ is symmetric under complex conjugation.

Since $\det[\Psi(x;\lambda)] = 1$, the spectrum $\sigma(q)$ can be completely characterized in terms of the trace of the transfer matrix $\Psi(L;\lambda)$ across one period; this is the *Floquet discriminant*,

$$\Delta(\lambda; q) = \mathrm{Tr}[\Psi(L;\lambda)], \tag{8}$$

which is a complex analytic function of λ. Then

$$\sigma(q) = \{\lambda \in \mathbb{C} \mid \Delta \in \mathbb{R},\ -2 \le \Delta \le 2\}.$$

Within the spectrum is a discrete set of points at which $\Delta = \pm 2$, called the *periodic spectrum*. It may include *simple points*, at which $d\Delta/d\lambda \neq 0$, or points of higher multiplicity. The endpoint of any band of spectrum must be a simple point; the *finite-gap* potentials are those with a finite number of simple points. All finite-gap solutions to the NLS may be explicitly given in terms of theta functions on the Jacobian of a hyperelliptic Riemann surface branched at the simple points of the periodic spectrum; see [2] for an exposition of this procedure.

For example, suppose γ is a m-times covered circle of diameter $1/a$. The discriminant is readily computed as

$$\Delta(\lambda; a) = 2\cos(\sqrt{a^2+\lambda^2}L), \qquad L = m\pi/a. \tag{9}$$

It follows that the Floquet spectrum of a multiply covered circle possesses continuous bands given by the union of the real axis and the imaginary interval $(-ia, ia)$ (see Figure 1). The periodic spectrum consists of

1. simple points $\lambda = \pm ia$;
2. an infinite number of real double points $\lambda = \pm\sqrt{n^2-m^2}\pi/L$, $n > m$;
3. the origin, which has multiplicity four;
4. $m-1$ pure imaginary double points $\lambda_j = i\sqrt{m^2-j^2}\pi/L$, $0 < j < m$, and their complex conjugates, which are associated with linear instabilities of the potential.[1]

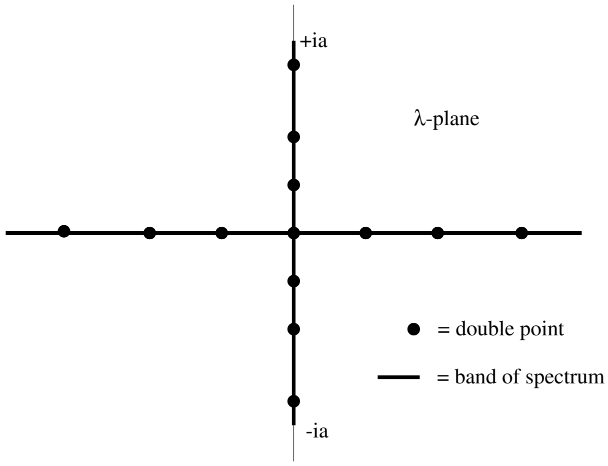

FIGURE 1. The Floquet spectrum of a plane wave potential with three unstable modes. The corresponding curve is a triply covered circle.

Note that a closed curve of length L does not necessarily generate a periodic potential; all we are assured of is that

$$q(x+L) = e^{i\varphi}q(x)$$

for some real constant φ, equal to the integral of the torsion over the curve. In this case, we say q is quasiperiodic.

The problem of characterizing those quasiperiodic potentials which correspond to closed curves has been solved by Grinevich and Schmidt [8]. First, they note that q may be replaced by its 'periodicized' version

[1] One can easily show this by studying the linear stability of $q(x)$ by means of a Fourier expansion.

$\tilde{q}(x) = e^{-i\phi x/L} q(x)$, and that the curve obtained from q using the reconstruction formula (5) at $\lambda = 0$ is identical to the curve obtained from $\tilde{q}$ using the solution of the linear system at $\lambda = \phi/L$.

So, we may assume q is L-periodic, and ask when the curve obtained via (5) at $\lambda = \Lambda_0$ is closed of length L. The answer may be given in terms of the spectrum of q. According to [8], necessary and sufficient conditions are that

(a) Λ_0 is a real point of the periodic spectrum, of multiplicity at least two—this much guarantees periodicity of the tangent vector to the curve;

(b) Λ_0 is a zero of the quasimomentum differential $dp(\lambda)$.

Using the definition of dp in terms of the Floquet eigenvalues (see [8]), one computes

$$\frac{dp}{d\lambda} = \frac{d\Delta/d\lambda}{\sqrt{\Delta^2 - 4}}.$$

Using an expansion of Δ near $\lambda = \Lambda_0$, it follows that the above two conditions are equivalent to Λ_0 being a periodic point of multiplicity at least 4.

As an addendum to the Grinevich-Schmidt closure conditions, we offer the following

Proposition 3.1. Suppose two complex-conjugate bands of the spectrum branch off in transverse directions from a band along the real axis at a multiple point $\lambda = \Lambda_0$; then this is a periodic point of multiplicity at least 4.

Proof. Without loss of generality we may assume $\Delta(\Lambda_0) = 2$. Since this is a strict local maximum of $\delta = \Re(\Delta)$, its Hessian is negative semidefinite there. However, since δ is also a harmonic function, its Hessian must vanish at Λ_0. Appealing to the Taylor series of the nonnegative function $2 - \delta$ along the real axis, we see that it must vanish at Λ_0 to order at least four. $\square$

We conclude this section by noting that more subtle geometric properties of the space curve γ may be derived from its spectrum, as exemplified by the following

Theorem 1. Suppose the spectrum of a finite-gap solution to NLS has six simple points, and is symmetric about the imaginary axis as well as the real axis. Then the corresponding solution $\gamma(x,t)$ to the filament flow is self-intersecting at each time.

The proof of this theorem, to be given in [4], relies on the representation of the curve in terms of theta functions on a hyperelliptic Riemann surface of genus 2. It is not true for genus one (four simple points), and we do not know if it generalizes to higher genus (i.e., more simple points).

4. Perturbing multiply covered circles

In this section we consider a complex periodic perturbation of the plane wave potential

$$q(x) = a + \epsilon[e^{i\theta_1}\cos(\mu x) + re^{i\theta_2}\sin(\mu x)] = q_0 + \epsilon q_1, \tag{10}$$

where r, θ_1, θ_2 are real parameters and μ is a real frequency. The effect of such perturbations on the spectrum of the plane wave potential were studied by Ablowitz, Herbst and Schober [1]. When the period of q_0 is taken to be $mL = m\pi/a$, then a perturbation with frequency $\mu = \mu_j = 2\pi j/L$, $1 \le \mu \le m-1$, causes the j-th complex double point to split into two simple points and either a gap in the spectrum or a transverse complex band of spectrum appears. The perturbation parameters govern the symmetry of the solution: if $\theta_1 = \theta_2 + n\pi$, or if $r = 0$, then the perturbed spectrum exhibits the symmetry $\lambda \to -\lambda$, and is consequently also symmetric about the imaginary axis. (This is due to the potential being an even or odd function of $x - c$; such symmetry is commonly imposed in the study of perturbations of the NLS equation.) On the other hand, if θ_1 and θ_2 are generic, then the perturbation will cause the selected complex double point to split asymmetrically in the complex plane.

Analytic dependence on $q(x) = q_0 + \epsilon q_1$ for the solution matrix of (4) gives an expansion of the form

$$\Psi = \Psi_0 + \epsilon\Psi_1 + \epsilon^2\Psi_2 + \dots, \tag{11}$$

where Ψ_0 is the fundamental matrix associated to q_0, given by (7).

We obtain a sequence of inhomogeneous linear systems

$$\frac{d\Psi_k}{dx} - \begin{pmatrix} i\lambda & q_0 \\ -\bar{q}_0 & -i\lambda \end{pmatrix}\Psi_k = Q_1\Psi_{k-1}, \qquad Q_1 = \begin{pmatrix} 0 & q_1 \\ -\bar{q}_1 & 0 \end{pmatrix} \tag{12}$$

for $k \ge 1$, which can be solved recursively using variation of parameters: if $\Psi_k(x) = \Psi_0(x)B_k(x)$ then

$$B_k(x) = \int_0^x \Psi_0^{-1}(t)Q_1(t)\Psi_{k-1}(t)\,dt. \tag{13}$$

(We normalize $\Psi_k(0) = 0$ for $k \ge 1$.)

Using the fact that q_1 has average value zero, we find that the Floquet discriminant is only perturbed at $O(\epsilon^2)$:

$$\Delta(\lambda; L) = \mathrm{Tr}(\Psi(\mathrm{L})) = 2\cos(kL) + \epsilon^2\mathrm{Tr}\left(\Psi_0(L)\int_0^L \Psi_0(t)^{-1}Q_1(t)\Psi_1(t)\,dt\right) + O(\epsilon^3).$$

It is not surprising, then, that the perturbed curve

$$\gamma(x; 0) = \gamma_0 + \epsilon\gamma_1 + O(\epsilon^2),$$

calculated using the reconstruction formula (5) with $\lambda = 0$, turns out to be closed up to $O(\epsilon^2)$; this will follow from the calculation in the next section.

The Floquet spectrum of the potential $q(x) = q_0 + \epsilon q_1(x)$ can be used to describe the knot type of the truncated curve $\gamma_c = \gamma_0 + \epsilon\gamma_1$. Consider the arclength reparametrization $\tilde{\gamma}$ of the truncated closed curve γ_c. A simple perturbation computation of its image under the Hasimoto map shows that the resulting complex potential $\tilde{q}$ agrees with $q = q_0 + \epsilon q_1$ up to terms of second order in ϵ. Since the Floquet spectrum depends analytically on the potential, then the Floquet spectra associated with q and $\tilde{q}$ are the same up to $O(\epsilon^2)$. Since $\tilde{\gamma}$ and γ_c have the same topology (being one a reparametrization of the other), then the Floquet spectrum of the original perturbed potential $q_0 + \epsilon q_1$ can be used to describe the knot type of γ_c. Summarizing we have:

Proposition 4.1. Given an isoperiodic deformation of the Floquet spectrum of a multiply covered circle within the class of finite-gap solutions, there exists a nearby spectral deformation which is associated to a quasi-periodic potential and which corresponds to a closed curve of periodic curvature and torsion (with $\int_0^{mL} \tau(s)\, ds \neq 0$ in general), whose knot type can be explicitely described in terms of the Floquet spectrum.

5. Torus knots

In this section we will show, by explicit calculation, that the generic first-order perturbation of the m-times covered circle is a torus knot of a type determined by the double point selected by the perturbation frequency. Before stating this result precisely, it is convenient to rewrite the perturbation term q_1 in terms of its real and imaginary parts. Since perturbations with $\Re(q_1) = 0$ cause the spectrum to be symmetric and the curves to be self-intersecting, we will assume the $\Re(q_1) \neq 0$. By absorbing a constant into ϵ, we may normalize the real part to have amplitude one, and write

$$q_1 = \cos(\mu x - \phi) + i\rho\cos(\mu x), \qquad \rho \in \mathbb{R}. \tag{14}$$

Note that we may assume $0 \leq \phi < \pi$, since any phase shift by π may be absorbed by translation in x and changing the sign of ρ.

Theorem 2. Suppose $\phi \neq 0$, $\rho \neq 0$, and $\mu = \mu_j$ with j relatively prime to m. Then for ϵ sufficiently small the curve $\gamma = \gamma_0 + \epsilon\gamma_1$ is a torus knot of type $(m, \pm j)$, where the sign is the opposite of that of ρ.

In identifying torus knot types, we take the following convention: a knot of type (p, q) travels p times around the torus the long way before closing up, whilst wrapping around the torus $|q|$ times the short way, forming a right-handed helix along the surface of the torus if $q > 0$ or left-handed if $q < 0$.

In terms of homoclinic orbits of multiply covered circles, the above theorem implies that the self-intersecting curve generated by a single Bäcklund transformation of an m-covered circle performed at the j-th complex double point separates two (m, j)-torus knots of opposite handedness.

Proof. Fix $a = 1$ for the remainder of the calculation. The Frenet frame of the circle is given by

$$\mathbf{t}_0 = \mathbf{e}_1 \cos 2x + \mathbf{e}_2 \sin 2x, \qquad \mathbf{n}_0 = \mathbf{e}_2 \cos 2x - \mathbf{e}_1 \sin 2x, \qquad \mathbf{b}_0 = \mathbf{e}_3.$$

Inserting the expansion (11) into formula (6) for the tangent vector gives

$$\mathbf{t} = \mathbf{t}_0 + \epsilon \left. [\mathbf{t}_0, B_1] \right|_{\lambda=0} . \tag{15}$$

Inserting the explicit form (7) for Ψ_0 into the formula (13) for B_1, we obtain by integration

$$B_1 = \rho \frac{2(\cos 2x \cos \mu x - 1) + \mu \sin 2x \sin \mu x}{4 - \mu^2} \mathbf{e}_1 + \rho \frac{2 \sin 2x \cos \mu x - \mu \cos 2x \sin \mu x}{4 - \mu^2} \mathbf{e}_2 - \frac{\sin(\mu x - \phi) + \sin \phi}{\mu} \mathbf{e}_3.$$

Computing the Lie bracket in (15) gives

$$\mathbf{t} = \mathbf{t}_0 + 2\epsilon \frac{\sin(\mu x - \phi) + \sin \phi}{\mu} \mathbf{n}_0 + 2\epsilon\rho \frac{2 \sin 2x - \mu \sin \mu x}{4 - \mu^2} \mathbf{b}_0.$$

We may obtain γ by using integration by parts on the second term, bearing in mind the Frenet equations satisfied by $\mathbf{t}_0$ and $\mathbf{n}_0$. A short calculation yields the periodic curve

$$\gamma = \gamma_0 - 2\epsilon\rho \frac{\cos 2x}{4 - \mu^2} \mathbf{b}_0 + 2\epsilon \frac{\cos(\mu x - \phi)\mathbf{n}_0 + \rho \cos(\mu x)\mathbf{b}_0}{4 - \mu^2} + \epsilon \frac{4(\sin(\mu x - \phi) + \sin \phi) - \mu^2 \sin \phi}{\mu(4 - \mu^2)} \mathbf{t}_0. \tag{16}$$

Taken together, the first two terms represent a shear performed on the circle, with vertical displacement proportional to ϵ times the $\mathbf{e}_2$-coordinate of the circle. (This shear is visible, for example, in the overall shape of the trefoil knot in Figure 3.) In the next group,

$$\cos(\mu x - \phi)\mathbf{n}_0 + \rho \cos(\mu x)\mathbf{b}_0 = \cos(\mu x - \phi) \left(\mathbf{n}_0 - \rho \cos \phi \mathbf{b}_0\right) - \rho \sin(\mu x - \phi) \sin \phi \mathbf{b}_0$$

shows that γ winds around γ_0 in the rectifying plane spanned by $\mathbf{n}_0$ and $\mathbf{b}_0$, tracing a sheared ellipse in a right-handed manner if $\rho < 0$ and left-handed if $\rho > 0$. The final term in (16) is a displacement, along the tangent direction of the circle, which is proportional to ϵ, and hence is not relevant to the knot type. Of course, the frequency $\mu = \mu_j$ causes γ to wind around γ_0 a total of j times before closing up. (If $d = \gcd(m, j) > 1$ then γ is a d-fold cover of a $(m/d, j/d)$ torus knot.) $\square$

We remark that, even if q_1 is a linear combination of terms of frequency μ_j for more than one value of j, the linearity in q_1 of equations (13) for B_1 and (15) for $\mathbf{t}$ guarantees that γ will be closed to first order in ϵ.

6. Experiments

In this section, we show several interesting cases of closed curves obtained by truncating the perturbation expansion (11) at order ϵ and using the Sym-Pohlmeyer reconstruction formula (5). Each of the curves shown are perturbations of an m-fold covered circle. They illustrate the relationships, discussed in previous sections, between their knot types and the Floquet spectrum of the corresponding NLS potentials.

Even perturbations: If q_1 is an even or odd function of x translated by a constant, corresponding to $r = 0$ or $\theta_1 = \theta_2$ or $\theta_1 = \theta_2 + \pi$ in (10), then the complex double points affected by the perturbation form cross or gap configurations which must be invariant under reflection in the imaginary axis. When the perturbation splits only one complex double point, the corresponding curves are self-intersecting, in accordance with Theorem 1.

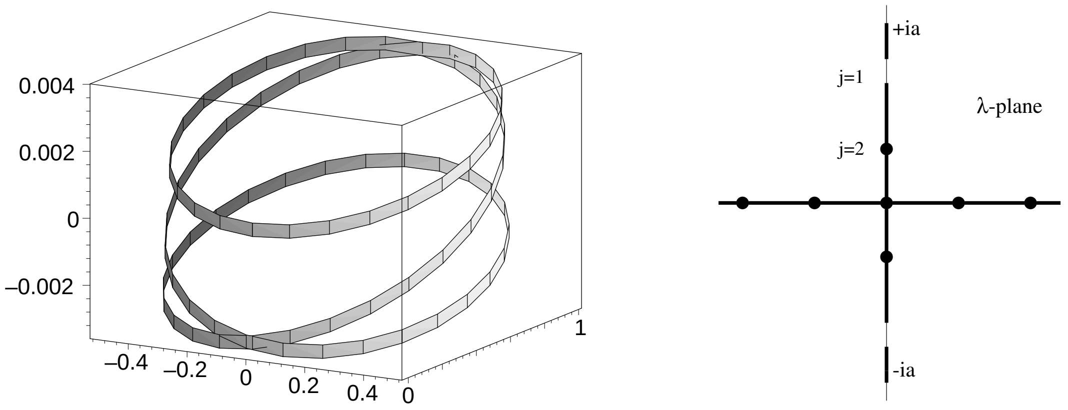

FIGURE 2. A self-intersecting curve arising from an even perturbation: $m = 3$, $j = 1$, $\rho = .2$, $\phi = 0$, $\epsilon = .02$ in (14).

Noneven perturbations, single mode: For generic values of r, θ_1, θ_2 in (10), the corresponding curves are not self-intersecting, and, in accordance with Theorem 2, torus knots of type (m, j) or $(m, -j)$ arise. These are shown in figures 3 and 4, with $j = 2$ in both cases. In each case the perturbation resonates with the

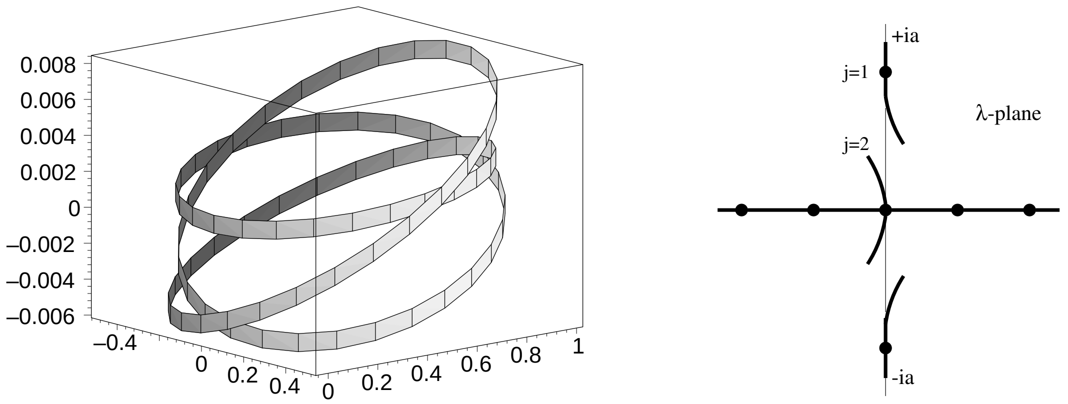

FIGURE 3. A left-handed trefoil and its spectrum: $m = 3$, $j = 2$, $\rho = .2$, $\phi = \pi/4$, $\epsilon = .02$.

second unstable mode $\exp(4\pi i/L)$, and causes the top part of the imaginary band to move within the first or second quadrant of the complex plane, depending on the sign of ρ in (14), and causes a gap to open up in the spectrum. In [1], it is observed that the two asymmetric spectral configurations are associated with initial conditions for modulated right and left travelling wave solutions. The handedness of the knot is thus related to the sign of the velocity of such potentials.

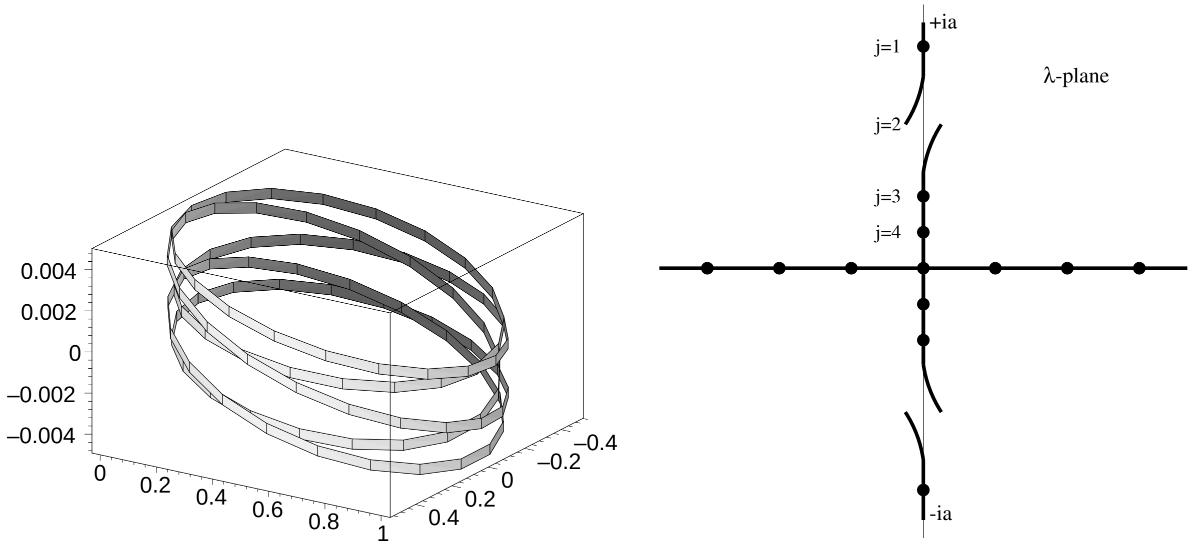

FIGURE 4. A right-handed $(5,2)$-torus knot ($m = 5$, $j = 2$, $\rho = -.2$, $\phi = \pi/4$, $\epsilon = .1$), and the Floquet spectrum of the corresponding NLS potential (the initial condition for a modulated left-travelling wave).

Noneven perturbations, two modes: Suppose we use a periodic perturbation of the form

$$q_1 = w_j\left(\cos(\mu_j x - \phi_j) + i\rho_j \cos\mu_j x\right) + w_k\left(\cos(\mu_k x - \phi_k) + i\rho_k \cos\mu_k x\right), \tag{17}$$

where j and k are integers labeling two distinct double points associated with unstable modes of the m-fold covered circle, μ_j, μ_k are the corresponding frequencies, and w_j, w_k are real weights. When both j and k are relatively prime to m, we expect that when $w_j \ll w_k$ (respectively, $w_k \ll w_j$) the truncated curve takes the form of an $(m, \pm k)$ (resp., $(m, \pm j)$) torus knot.

However, suppose $d = gcd(j,m)$ is greater than one, and $gcd(d,k) = 1$. Then we observe that:

> for w_k/w_j sufficiently small, the curve has the knot type of a *cable knot*, with companion an $(m/d, \pm j/d)$ torus knot, patterned on a $(d, \pm k)$ torus knot, where the signs are determined by ρ_j and ρ_k in accordance with Theorem 2.

The terminology is standard in knot theory (see [10]): the 'pattern' is regarded as an embedding of a loop into a solid torus, and then this embedding is composed with an embedding of the solid torus into a thickened neighbourhood of the companion knot. For example, in Figure 5 we see a result for the choices $m = 6, j = 4$

and $k = 5$: a cable built on the companion $(3,-2)$ (left-handed trefoil) knot, patterned on a $(2,5)$ torus knot. Of course, the knot type of cable depends on that of the pattern *within* the solid torus. For example,

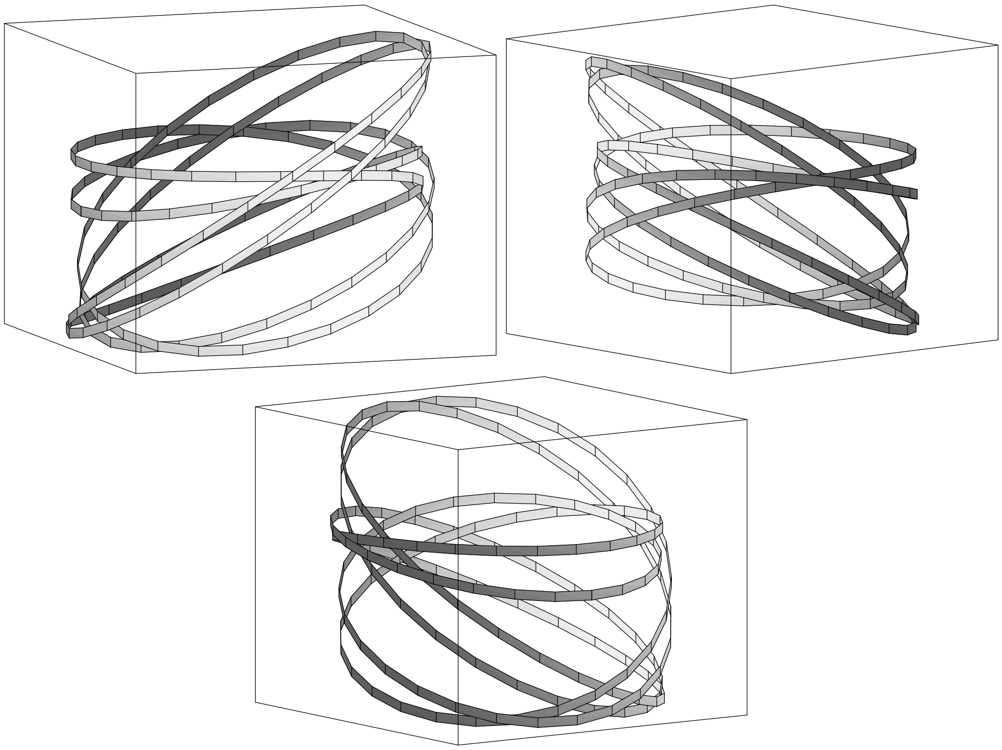

FIGURE 5. Three views of a cable knot, obtained using perturbation (17) with $m = 6, j = 4, k = 5$, $w_j = 1$, $w_k = 0.1$, $\phi_j = \phi_k = \pi/2$, $\rho_j = .2$, $\rho_k = -.3$ and $\epsilon = 0.02$.

if we had chosen $k = 1$ instead, the pattern is unknotted but nevertheless represents a nontrivial loop in the solid torus; the resulting cable knot is known as a two-stranded cable on the trefoil.

Acknowledgements

The first author is partially supported by NSF grant DMS-9705005. All figures were produced using Maple V.

References

1. M.J. Ablowitz, B.M. Herbst, C.M. Schober, Computational chaos in the nonlinear Schrödinger equation without homoclinic crossings, *Physica A* 228 (1996), 212-235.
2. E.D. Belokolos, A.I. Bobenko, V.Z. Enol'skii, A.R. Its, V.B. Matveev, Algebro-Geometric Approach to Nonlinear Integrable Equations, Springer (1994).
3. A. Calini, A note on a Bäcklund transformation for the continuous Heisenberg model, *Phys. Lett.* A 203 (1995), 333-344.
4. A. Calini, T. Ivey, Finite-genus solutions of the Vortex Filament Equation, *in preparation.*
5. A. Calini, T. Ivey, Knot types, Floquet spectra and finite-gap solutions of the vortex filament equation, preprint (1999).

6. A. Doliwa, P. M. Santini, An elementary geometric characterization of the integrable motion of a curve. *Physics Letters A*, 185 (1994), 373-384.
7. Y. Fukumoto, R.L. Ricca, *Vortex Filament Motion and Related Integrable Systems*, World Scientific, (1999).
8. P.G. Grinevich, M.U. Schmidt, Closed curves in $\mathbf{R}^3$: a characterization in terms of curvature and torsion, the Hasimoto map and periodic solutions of the Filament Equation. *preprint dg-ga/9703020* (1987).
9. H. Hasimoto, A soliton on a vortex filament, *J. Fluid Mech.*,51 , 1972, pp. 477–485.
10. W.B.R. Lickorish, *An Introduction to Knot Theory*, Springer 1997.
11. A. Sym, Soliton surfaces and their applications, in: *Geometrical aspects of the Einstein equations and integrable systems*, Lecture Notes in Physics, 239 (1985), 154.
12. V.E. Zakharov and A.B. Shabat, Exact theory of two-dimensional self-focusing and one-dimensional self-modulation of waves in nonlinear media. *Soviet Phys. Jetp* **34** (1972) 62–69.